SUPPLEMENTAL MATERIAL

Expanded Methods

Plasmids and retroviral or lentivirus constructs. The small double-stranded hairpin shRNAs targeting SOX17 were designed by BLOCK-iT RNAi Designer (Invitrogen), synthesized by Integrated DNA Technologies (IDT), and inserted into a pLL3.7 lentiviral vector [1]. The sequences of SOX17 shRNAs were SOX17-1: GGACCGCACGGAATTTGAA; SOX17-2: GCATGACTCCGGTGTGAAT; SOX17-3: CCGCGGTATATTACTGCAA. Lipofectamine 2000 was used to transfect pLL3.7 lentiviral vector to HEK293T cells (seed 2.0×10^6/6-well dish 1 day prior). The medium containing lentiviruses was collected and filtered 2 days after transfection. The iECs was incubated with the virus cocktail supplemented with 8μg/ml polybrene for 6-8hr. To overexpress SOX17 and distinguish overexpressed genes from endogenous gene expression, full-length SOX17 (pMXs-SOX17) plasmids were purchased from Addgene (Cat: 50781 and 50782 respectively). To package retrovirus expressing SOX17, Fugene HD transfection reagent (Roche, E2311) was used to transfect PLAT-A cells (1.0×10^6 / 6-well dish). The medium containing the retrovirus was collected and filtered 2 days after transfection. For SOX17, over-expression studies, iECs were incubated with a virus cocktail supplemented with 4μg/ml polybrene for 6-8hr.

Quantitative real-time PCR. Total RNA was extracted using the PureLink RNA Mini Kit (Ambion) according to manufacturer's protocol. cDNA was synthesized by High Capacity cDNA Reverse Transcription Kit (Applied Bipsystems). 50ng cDNA (relative to RNA amount) was amplified by real-time PCR. FastStart Universal SYBR Green Mastermix (Roche) was used for quantitative real-time PCR. TaqMan® Gene Expression Assays

from Applied Biosystems were used to detect human hemoglobin beta and human hemoglobin gamma with the primer/probe sets of hemoglobin beta (Hs00747223_g1) and hemoglobin gamma (Hs00361131_g1), respectively, while GAPDH (Hs02758991_g1) served as control. The sequences of qPCR primers are shown as following:

Human	*B2M`*	Forward	5'- ATAAGTGGAGGCGTCGCGCTG
		Reverse	5'- ACAGCTAAGGCCACGGAGCG
Human	*CD34*	Forward	5'- CCACAGGAGAAAGGCTGGGCG
		Reverse	5'- CCGGTCCCGTTTTCCTGAGCC
Human	*OCT4*	Forward	5'- AGAAGGATGTGGTCCGAGTGTG
		Reverse	5'- CATAGTCGCTGCTTGATCGC
Human	*c-MYC*	Forward	5'- AAGACAGCGGCAGCCCGAAC
		Reverse	5'- TGGGCGAGCTGCTGTCGTTG
Human	*NANOG*	Forward	5'- ACAACTGGCCGAAGAATAGCA
		Reverse	5'- GGTTCCCAGTCGGGTTCAC
Human	*VE-cadherin*	Forward	5'- GACCGGGAGAATATCTCAGAGT
		Reverse	5'- CATTGAACAACCGATGCGTGA
Human	*CD31*	Forward	5'- AACAGTGTTGACATGAAGAGCC
		Reverse	5'- TGTAAAACAGCACGTCATCCTT
Human	*FLK1*	Forward	5'- TCGAAGCATCAGCATAAGAAACTT
		Reverse	5'- GCCCACTGGATGCTGCA
Human	*VWF*	Forward	5'- GGGCTGCCAGAAACGCT
		Reverse	5'- CAAGATACACGGAGAGGCTCACT
Human	*SOX17*	Forward	5'- TCTGCCTCCTCCACGAAG
		Reverse	5'- ACGCCGAGTTGAGCAAGA
Human	*GATA1*	Forward	5'- ATCAAGCCCAAGCGAAGACT
		Reverse	5'- CATGGTCAGTGGCCTGTTAAC
Human	*PU.1*	Forward	5'- GGGGTGGAAGTCCCAGTAAT
		Reverse	5'- ACGGATCTATACCAACGCCA

Human	*RUNX1*	Forward	5’- AGAACCTCGAAGACATCGGC
		Reverse	5’- GGCTGAGGGTTAAAGGCAGTG

Flow cytometry. Cells were harvested from culture dishes and analyzed on the CyAn ADP instrument (Beckman Coulter) with Summit software 4.4. The antibodies used for flow cytometry analysis were CD34-PE (130-081-002, Miltenyi Biotec), Alexa Fluor 647 mouse anti-human CD144 (561567, BD Biosciences), FIFC anti-hCD31/PECAM-1 (FAB3567P, R&D Systems), Alexa Fluor 647 mouse anti-human CD309 (VEGFR-2) (560495, BD Biosciences), PE mouse anti-human CD106 (555647, BD Biosciences), and APC mouse anti-human CD62E (551144, BD Biosciences), APC mouse anti-human CD235a, (MACS 130-100-262), PE mouse anti-human CD235a (BD Biosciences 555570), PE mouse anti-human TRA-160 (eBioscience, 12-8863) , and PE mouse anti-human TRA-180 (eBioscience, 12-8883). Isotype controls were Alexa Fluor 647 mouse $IgG1_k$ (557714, BD Biosciences), Alexa Fluor 647 mouse $IgG1_k$ (557783, BD Biosciences), PE mouse $IgG1_k$ (554680, BD Pharmingen), PE mouse $IgG2b_k$ (555743, BD Biosciences). FITC mouse $IgG1_k$ (554008, BD Pharmingen) and APC mouse $IgG2a_k$ (555576, BD Biosciences). Cell proliferation was assayed by flow cytometry using the APC BrdU flow cytometry kit (51-9000019AK, BD Biosciences) according to manufacturer’s instructions.

Cytospin preparation and Hema 3 staining. Cells (10^5) were suspended in 300 ml and used for cytospin preparations with the Thermo Scientific Shandon 4 Cytospin kit. The slides were fixed and stained with Hema 3 kits (Fisher Scientific, 123-869) according to manufacturer’s protocol to visualize erythroblasts. The cells were imaged using a Zeiss ApoTome inverted microscope with 20×, 40× and0× objectives.

Erythroid Colony-Forming assay. MethCult™ H4034 Optimum with Recombinant Cytokines and EPO were purchased from Stemcell Technologies and colony forming assay to evaluate the colony-forming function of generated erythroblasts were performed according to the manufacturer instructions. Briefly, 3×10^3 induced erythroblasts or fibroblasts were collected, washed and then mixed in 3×1,300 µL MethCult™. The suspended cells were dispensed into petri-dishes using a syringe and blunt-end needle. The dishes were then incubated for 14 days in a humidified incubator at 37°C and 5% CO2. The erythroid colonies were evaluated and counted using an inverted microscope and gridded scoring dishes. The colonies were plucked for further assays.

Immunocytochemistry, immunohistochemistry and fluorescence microscopy. Immunocytochemistry was performed on cells after fixation with 4% paraformaldehyde. Fixed cells were permeabilized and blocked with 5% normal goat serum, 0.1% Triton X-100 in PBS for 30 min at RT [2]. Then the cells were incubated with primary antibodies for 2hr and secondary antibodies labeled with fluorescence Alexa488 and Alexa647 (Invitrogen, Carlsbad, CA) for 1hr. Immunohistochemistry was performed on paraffin-embedded sections after heat-induced antigen retrieval (30 min at 95ºC in 0.01M sodium citrate, pH6). The slides were permeabilized and blocked with 5% normal goat serum, 0.1% Triton X-100 in PBS for 1hr at RT. The slides were then incubated with primary antibody at 4ºC overnight. For immunofluorescence, fluorescent Alexa Fluor-488 and Alexa-568 (Invitrogen, Carlsbad, CA) labeled secondary antibodies were applied to identify the primary antibodies. The slides were mounted in ProLong Gold antifade reagent with DAPI (Invitrogen). Florescence images were acquired using Zeiss ApoTome microscope with 20×, 40× and 60× objectives. Confocal image acquisition was performed

using a Zeiss LSM 780 laser scanning microscope (Carl Zeiss Jena) with 20×, 40× and 60× water objectives. Primary antibodies used were mouse anti-human CD31 (M-0823, DAKO, Denmark), goat anti-VE-cadherin (Santa Cruz Biotech, SC-6458), rat anti-mouse TER-119/Erythroid cells (BD Pharmingen, 550565), mouse anti-human CD235a (Glycophorin A) (R&D Systems, MAB 1228), mouse anti-human CD235a (R&D Systems, MAB 1125).

Western blotting. Immunoblotting was performed as described [2]. The primary antibodies applied in Western blotting were mouse anti-actin (A2066, Sigma); goat anti-VE-cadherin (sc-6458, Santa Cruz); rabbit anti-FLK1 (VEGFR2) (2479, Cell Signaling Technology), mouse anti-human CD31 (M-0823, DAKO, Denmark), goat anti-human SOX17 (AF1924, R&D). Donkey horseradish peroxidase (HRP)-linked anti-goat, mouse and rabbit IgG (SantaCruz) were used as secondary antibodies. Signals were developed by enhanced chemiluminescence HRP substrate – SuperSignal West Femto Maximum Sensitivity Substrate (34095, Thermo Scientific) and detected with the LAS-3000 mini (Fuji).

Transendothelial electrical resistance measurements. Assessment of responses of iEC to inflammatory stimuli was performed by measuring thrombin-induced increase in endothelial permeability as described [3]. Human iECs and control human EC (5.0×10^4/ cm^2) were cultured on gelatin-coated gold electrodes for 1 day. The smaller electrode and larger counter electrode were connected to a phase-sensitive lock-in amplifier to monitor the voltage. A constant current of 1 μA was supplied by a 1 V, 4000 Hz AC signal connected serially to a 1MΩ resistor between the smaller electrode and the larger counter electrode. Before each experiment, confluent endothelial monolayers using both cell types were incubated in serum-free medium for 1hr. Thrombin (3.5μg/ml - 0.5 Units) was

added as indicated. The data are presented as a change in the resistive portion of electrical impedance normalized to its value at time 0.

Gene expression and bioinformatics. Gene expression data on fibroblasts, erythro-angioblasts derived from fibroblast de-differentiation, iECs, and adult human ECs were obtained using the Affymetrix GeneChip® Human Transcriptome Array 2.0. The analysis was performed in the R environment for statistical computing using the Affy and Limma packages. The 11 Affymetrix CEL files were pre-processed by Robust MultiChip Analysis. For each gene, the normalized intensity in each cell type was paired with the normalized intensity of the remaining samples and analyzed with the Limma package. A linear model was fitted to the design matrix for the samples using Limma, and differentially expressed genes identified for each pairwise comparison using a moderated *t* statistic, which applies an empirical Bayes method to borrow information across genes. P-values were adjusted for multiple testing using the Benjamini and Hochberg's method, which controls the false discovery rate. Gene expression profiles were visually depicted using heatmaps. Samples and genes were ordered by hierarchical clustering and represented by the dendrogram. The color bar indicates gene expression level in binary logarithm (log_2) scale. The blue to red color spectrum represented low to high expression levels.

Tube formation assay. A cell suspension containing 0.3×10^5/ well of either ECs (control) or iECs was placed on top of wells coated with Matrigel (10 mg/ml; BD Matrigel Basement Membrane Matrix, A6661) in a 24-well plate (Nunc). Rearrangement of cells and formation of capillary structures were observed at 24 hours.

Telomerase activity assay. Telomerase activity was determined using the telomeric repeat amplification protocol (TRAP). TRAP assay was performed using the TRAPeze

Telomerase Detection kit (Millipore) and a Cy5 fluorescently labeled TS primer according to established protocols [4]. Densitometry of telomerase-specific ladder and internal standard were quantified using ImageJ and used to calculate relative telomerase activity compared to an internal standard control.

In vivo staining of functional human and mouse vessels by lectins. Rhodamine-labeled Ulex Europaeus Agglutinin I (UEA I; vectorlabs, DL-1208 for staining human endothelium) and DyLight 649 labeled Griffonia Simplicifolia Lectin I isolectin B4 (GS-IB4, vectorlabs, RL-1062 for staining mouse endothelium) were mixed into saline with 1 mM CaCl2 solution as described [5]. The lectin mixture (50 μg of each/100 μL/mouse) [5] was injected intravenously 30 minutes before harvesting Matrigel implants or hearts. Quantification of vessel density in plugs and hearts was described as above.

Teratoma formation assay. 1×10^6 $CD34^+$ progenitor cells or iPSCs suspended in Matrigel were injected subcutaneously to the abdomen of anesthetized immune-deficient NOD-SCID mice (Jackson Laboratory, NOD.Cg-*Prkdc*^{scid} *Il2rg*^{tm1Wjl}/SzJ, strain 005557). The iPSCs were generated from reprogramming human BJ newborn foreskin fibroblasts (ATCC, Manassas, VA) using a protocol previously described. The mice were monitored for 8 weeks. The mice were sacrificed and teratomas or plugs were explanted at 8 weeks' post implantation. The teratoma were fixed in 10% formalin for 2 days and embedded in paraffin. Histological characterization of H&E staining slides was performed to identify the cells from all three germ layers.

Myocardial infarction surgery Anesthesia was introduced with 1.5-3% isoflurane inhalation in a closed glass chamber and Etomidate (10 mg/kg body weight IP). Mice were orally intubated with one 18G angiocath sleeve and artificially ventilated with a rodent

respirator (tidal volume 0.2-0.3ml (based on body weight), rate 135 strokes/min). Surgical anesthesia was maintained using 1% isoflurane delivered through a vaporizer with air connected in series to rodent ventilator. A dose of buprenorphine sustained release (0.1 mg/kg SC) was administered pre-operatively. Under microscopic view, left thoracotomy was performed by 1 cm careful incision along sternum and 1 mm to the left from a midline between the 2nd and 4th rib in layers (skin, pectoral muscles and ribs avoiding mammary arteries). Having the heart in view, the pericardium was removed to ligate the left main coronary artery with 8-0 prolene suture 1–2 mm below the ostium. The chest cavity was then closed in three layers: intercostal muscles-interruptive, pectoral muscles and skin-continuous with the 7-0 nylon sutures. The thorax was drained with a PE-10 cannula inserted into incision upon closure to evacuate the chest cavity and re-establish proper intrapleural pressure. After tube removal, mice were weaned from anesthesia and placed in the warming pad until ambulatory and then returned to the appropriate housing facility.

Transthoracic echocardiography. Evaluation of regional cardiac function based on LV thickness and morphology was performed by transthoracic echocardiography. Mice were anesthetized by 3.5% isoflurane and placed a heated platform (VisualSonics, Inc.) where ECG (lead II), heart rate, respiratory waveform and respiratory rate were monitored and displayed on the ultrasound's CPU display. Then, 3 views were recorded with the sample volume in the proper modes (B-mode, M-mode, pulsed Doppler or tissue Doppler): 1. The parasternal long axis [B-mode and/or M-mode]; 2. The parasternal short axis [M-mode was taken at the papillary level followed by tissue Doppler of the myocardium]; 3. Apical view [pulsed Doppler of the mitral flow]. Fractional shortening (FS) and ejection fraction (EF) were used as indices of cardiac contractile function. M-mode tracings were used to

measure LV internal diameter at end diastole (LVIDd) and end systole (LVIDs). FS was calculated according to the following formula: FS (%) = [(LVIDd − LVIDs)/LVIDd] × 100. EF is estimated from (LVEDV-LVESV)/LVEDV 100%. LVESV (left ventricular end systolic volume); LVEDV. (left ventricular end diastolic volume).

SUPPLEMENTAL TABLE

Supplemental Table 1: Cardiac function assessment by echocardiography

Echo index	Treatment	Before MI	Post MI 1 W	Post MI 2 W
Heart Rate (bpm)	Fib	443.99 ± 12.97	451.16 ± 27.41	455.33 ± 39.90
	$CD34^+$	443.90 ± 12.97	491.61 ± 28.93	449.93 ± 24.67
LV internal diameter at end systole (LVIDs)	Fib	2.12 ± 0.13	3.60 ± 0.37	3.79 ± 0.53
	$CD34^+$	2.01 ± 0.11	3.01 ± 0.27	3.46 ± 0.34
LV internal diameter at end diastole (LVIDd)	Fib	3.46 ± 0.11	4.56 ± 0.22	4.43 ± 0.27
	$CD34^+$	3.26 ± 0.09	4.06 ± 0.64	4.03 ± 0.84
LV End Systolic Volume (LVESV) (ul)	Fib	12.56 ± 3.19	62.91 ± 5.20	79.96 ± 13.07
	$CD34^+$	12.04 ± 3.27	34.55 ± 3.15 *	56.43 ± 5.60
LV End Diastolic Volume (LVEDV) (µl)	Fib	48.49 ± 5.15	99.51 ± 12.96	114.4 ± 11.19
	$CD34^+$	48.47 ± 5.95	70.29 ± 9.01 *	93.36 ± 13.59 *
Stroke Volume (µL)	Fib	35.74 ± 1.93	28.58 ± 3.49	24.49 ± 3.75
	$CD34^+$	36.96 ± 1.51	36.32 ± 2.45 *	37.58 ± 2.81 **
Ejection Fraction (%)	Fib	74.29 ± 2.36	35.19 ± 2.27	23.38 ± 2.39
	$CD34^+$	69.04 ± 3.13	52.05 ± 4.42 ***	43.50 ± 5.91 **
Fractional Shortening (%)	Fib	42.37 ± 5.29	16.07 ± 4.25	11.34 ± 3.89
	$CD34^+$	39.95 ± 1.95	27.00 ± 2.74 ***	25.66 ± 3.93 ***
Cardiac Output (ml/min)	Fib	15.12 ± 0.4	12.41 ± 2.0	10.20 ± 1.01
	$CD34^+$	15.57 ± 0.58	18.02 ± 1.2 **	15.80 ± 1.49 **
LV Mass (mg)	Fib	99.91 ± 7.24	155.20 ± 15.34	159.30 ± 16.67
	$CD34^+$	94.29 ± 8.19	112.00 ± 12.70 *	136.8 ± 9.47
LV Mass Corrected (mg)	Fib	70.60 ± 2.81	119.19 ± 11.10	131.48 ± 9.93
	$CD34^+$	70.59 ± 2.30	84.22 ± 24.53 *	86.18 ± 5.04 ***

Data are presented as mean ± SE. ***P<0.001, **P<0.01, *P<0.05, $CD34^+$ progenitors ($CD34^+$) treatment were compared to fibroblasts (Fib) treatment using repeated measures

two-way ANOVA.

Supplemental Figure 1

A

Fibroblasts

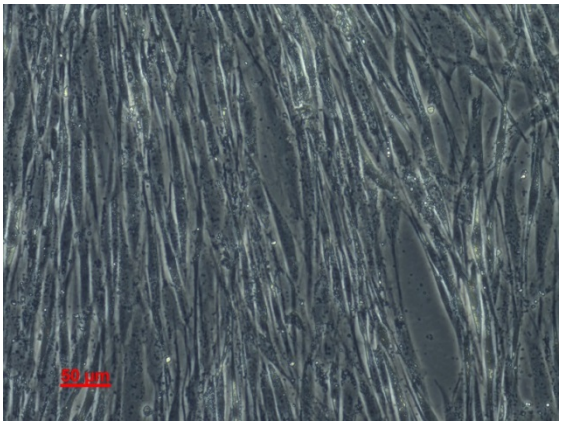

B

De-Differentiated
Fibroblasts at day 7

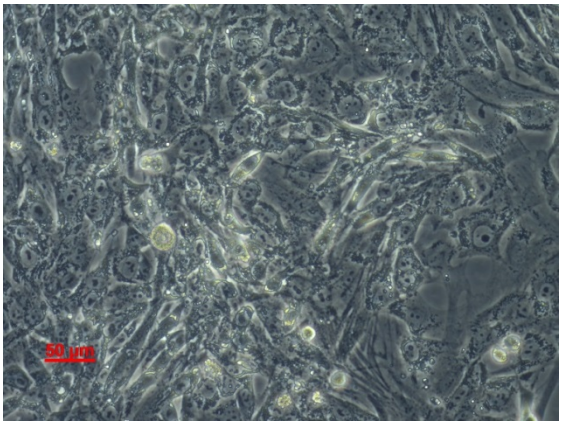

C

iECs at day 10

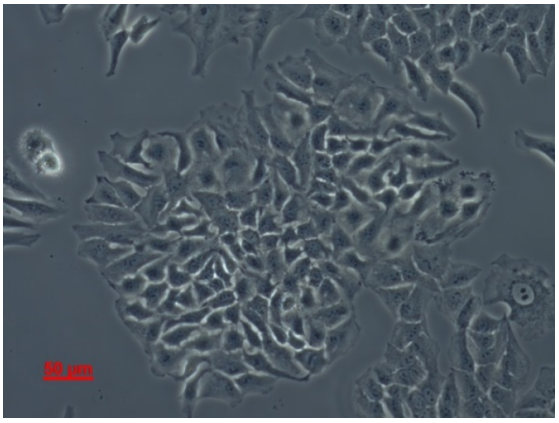

D

Induced Erythroblasts
at day 4

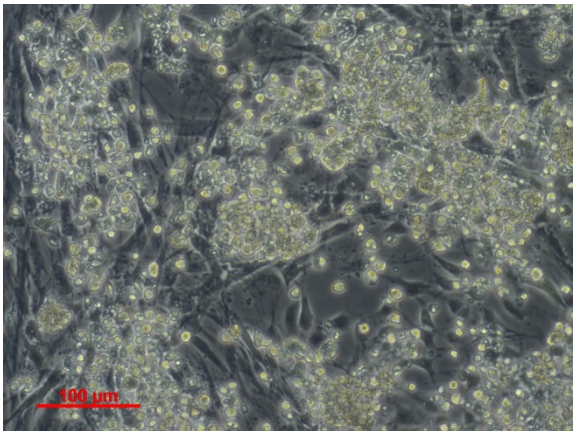

.

Supplemental Figure 2

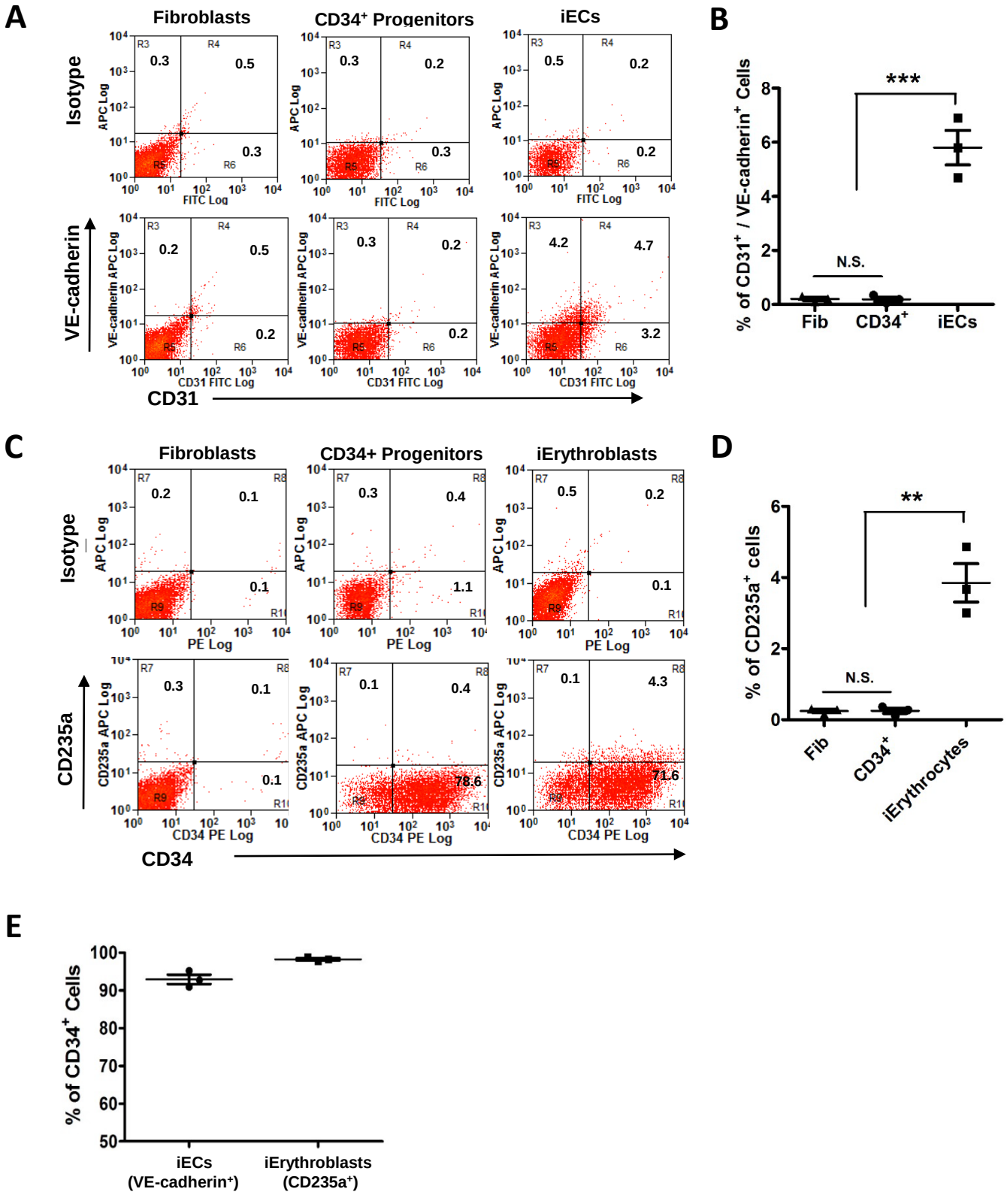

Supplemental Figure 3

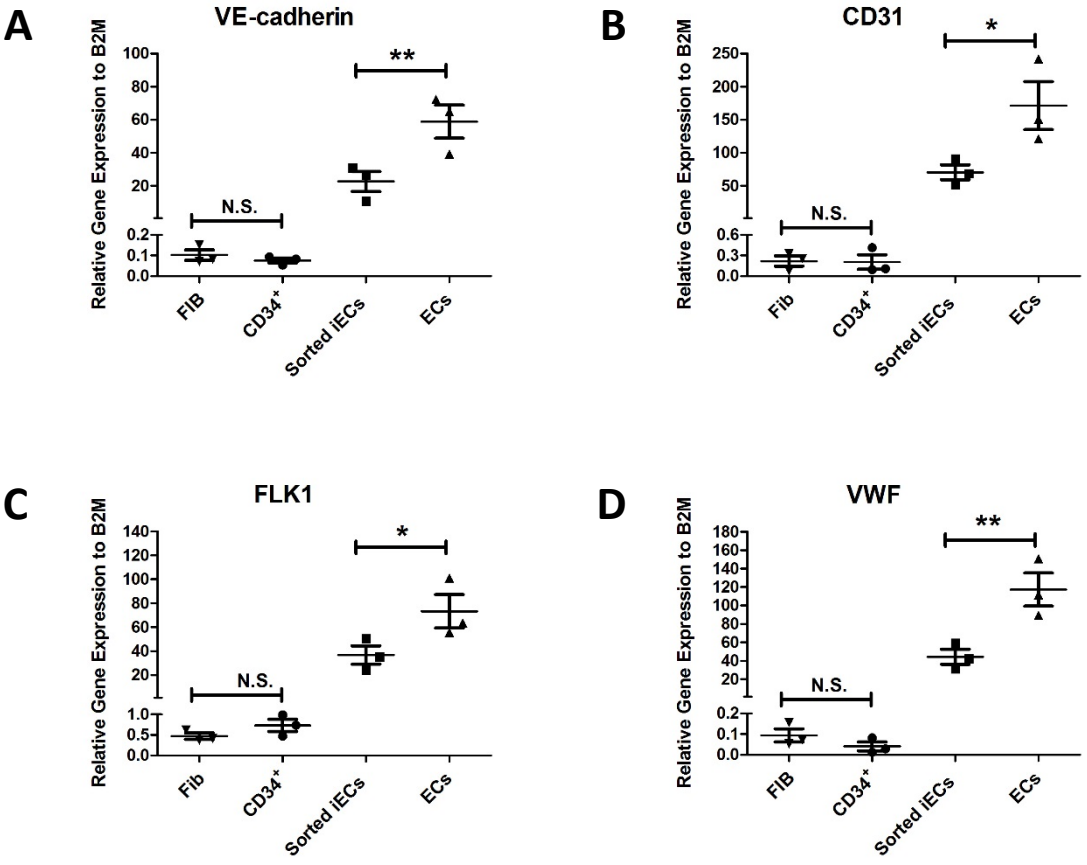

Supplemental Figure 4

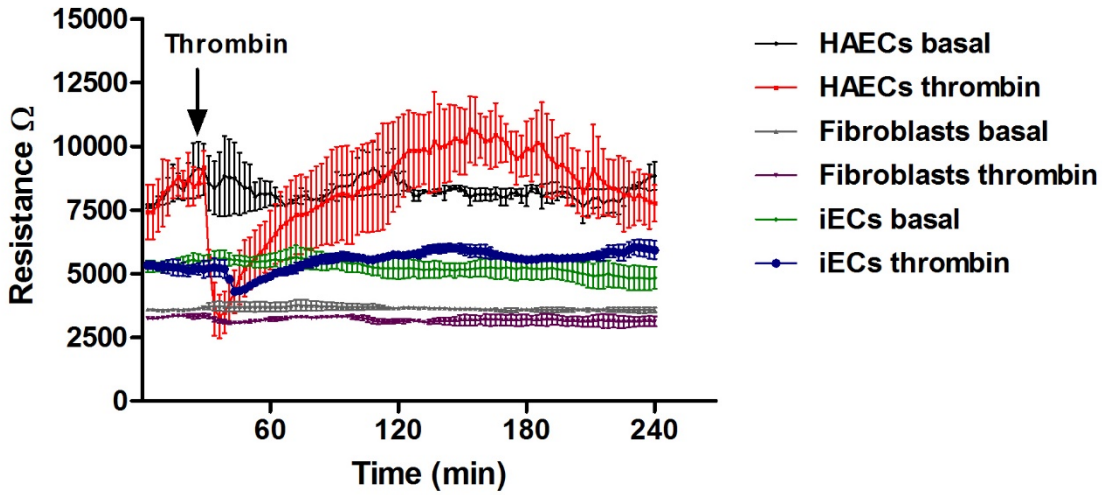

Supplemental Figure 5

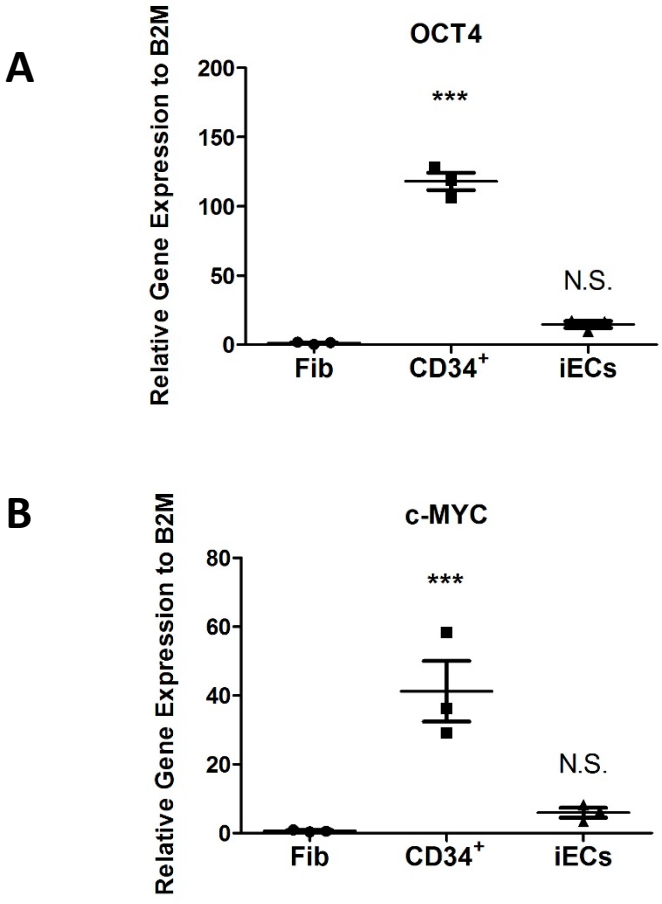

Supplemental Figure 6

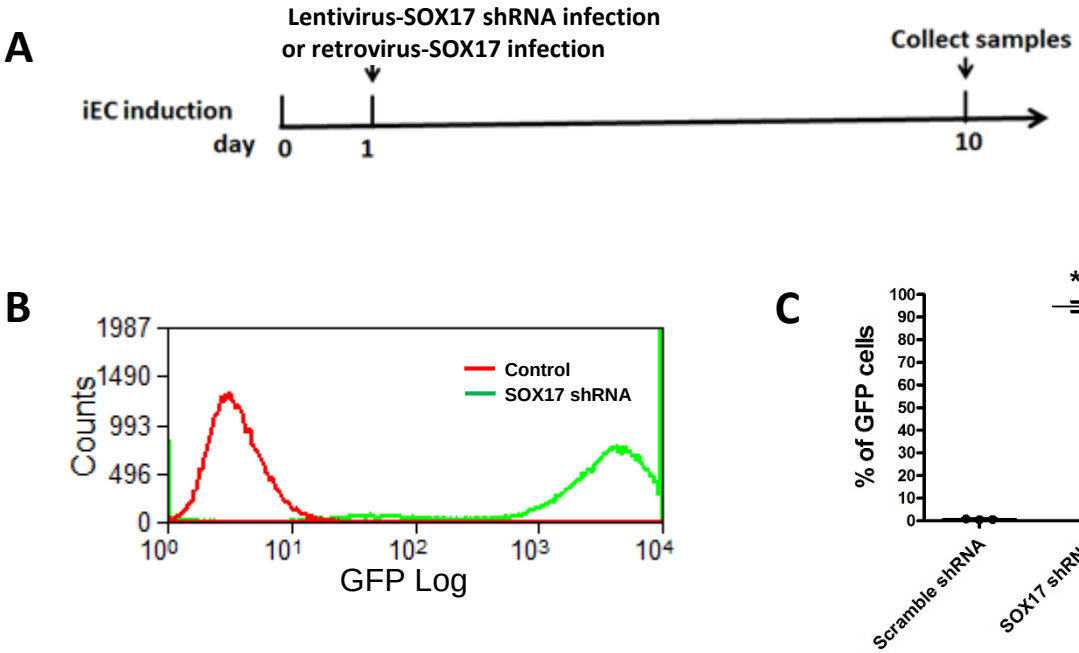

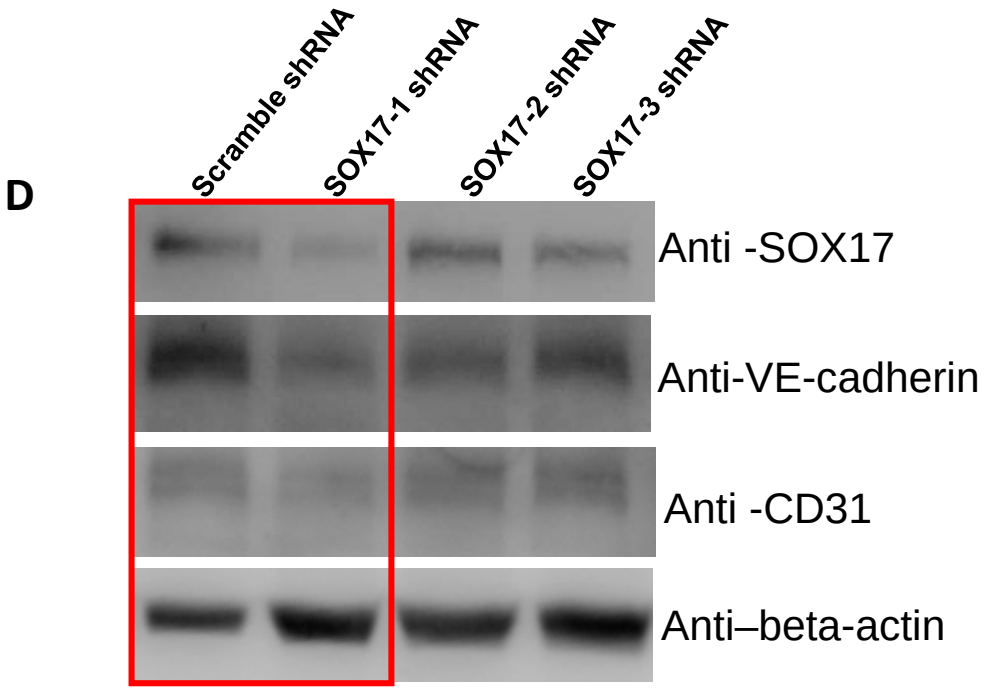

Supplemental Figure 7

A

Mouse CD31 / Mouse TER119 / DAPI

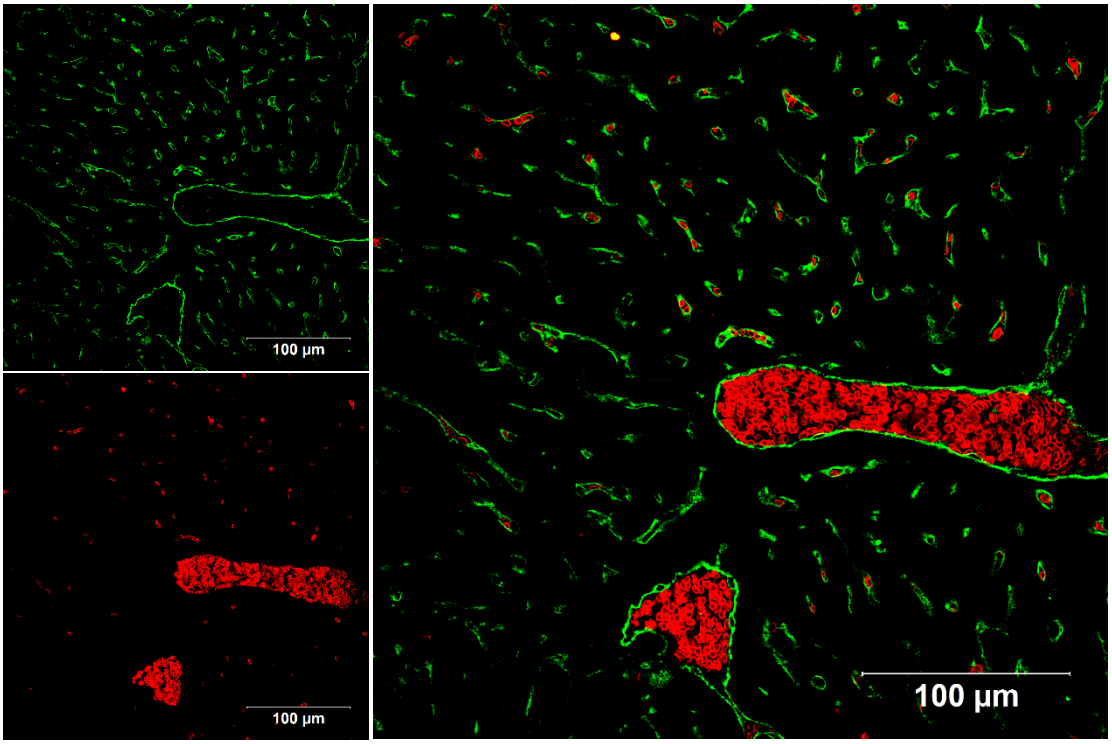

B

Mouse CD31 / Human CD235a / DAPI

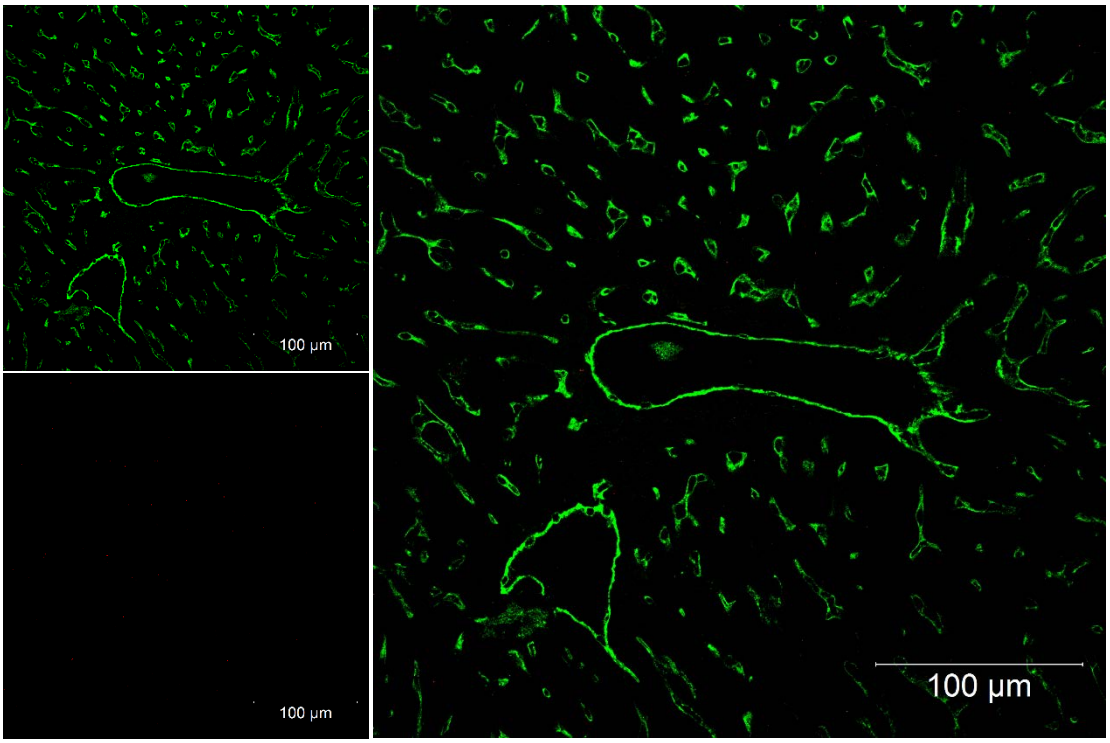

Supplemental Figure 8

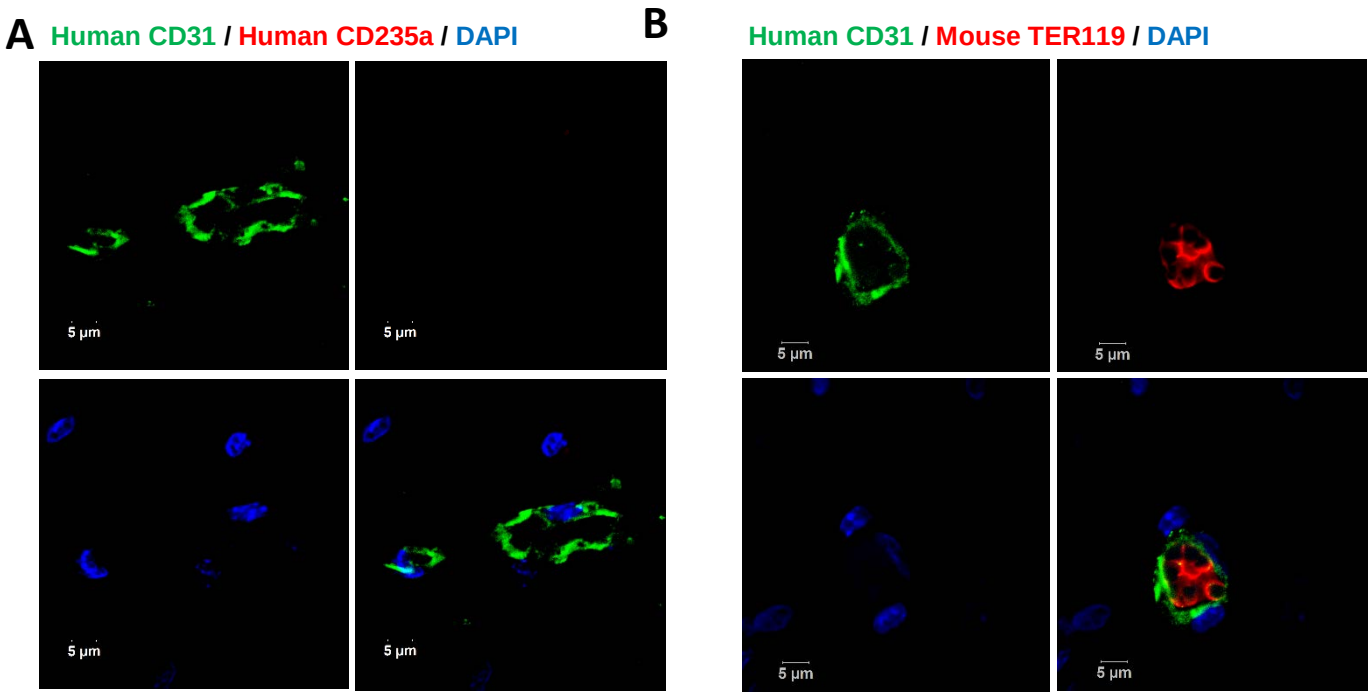

Supplemental Figure 9

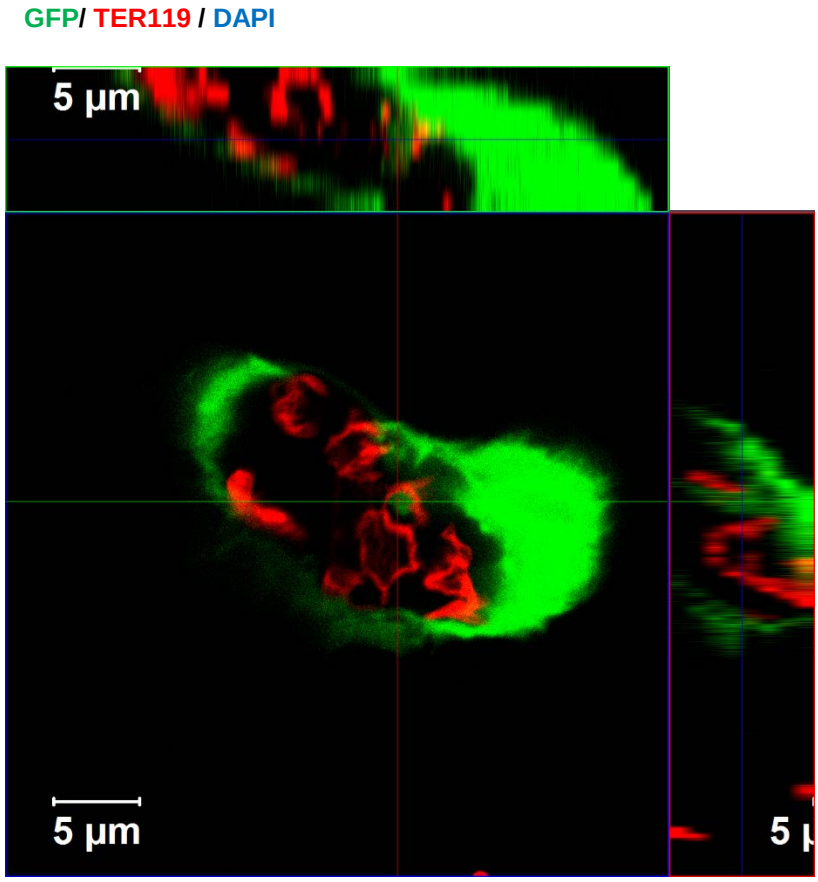

Supplemental Figure 10

A

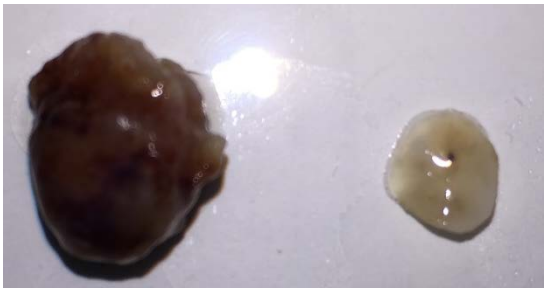

B

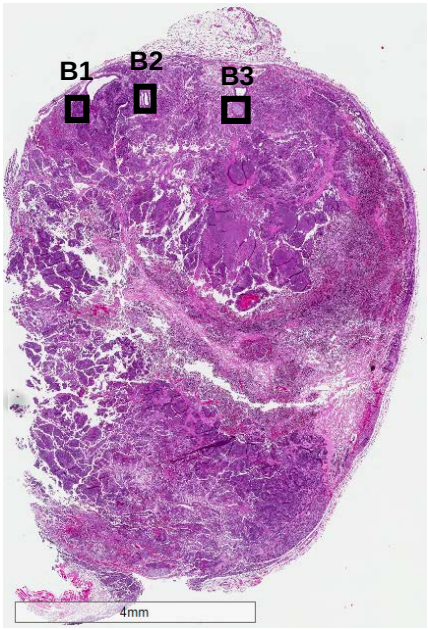

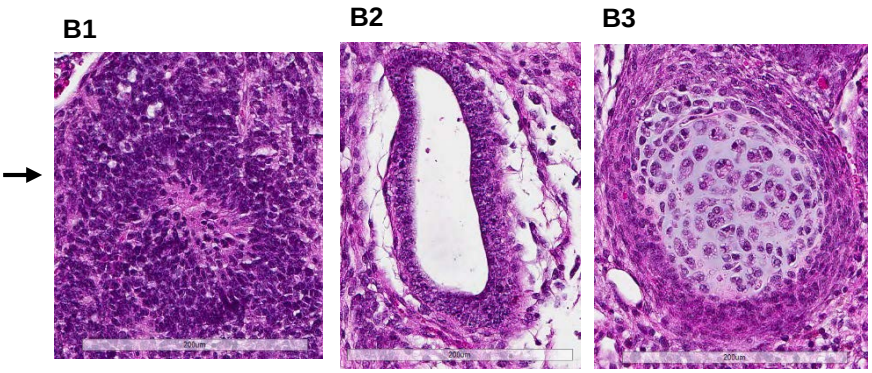

C

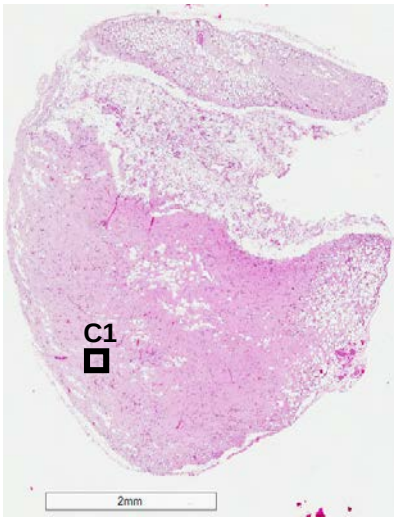

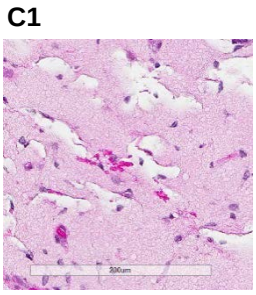

D

	Teratoma	Non-teratoma
iPSCs	5	0
CD34^{+} Progenitors	0	5
Fisher's exact test	P<0.01	

Supplemental Figure 11

A

GFP / Human CD31 / Mouse CD31 / DAPI

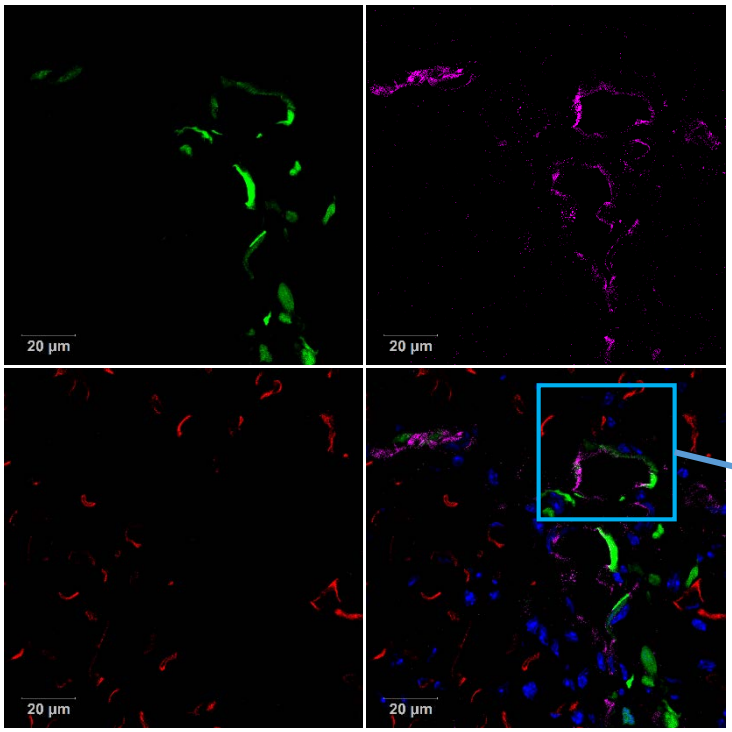

GFP / Human CD31 / Mouse CD31 / DAPI

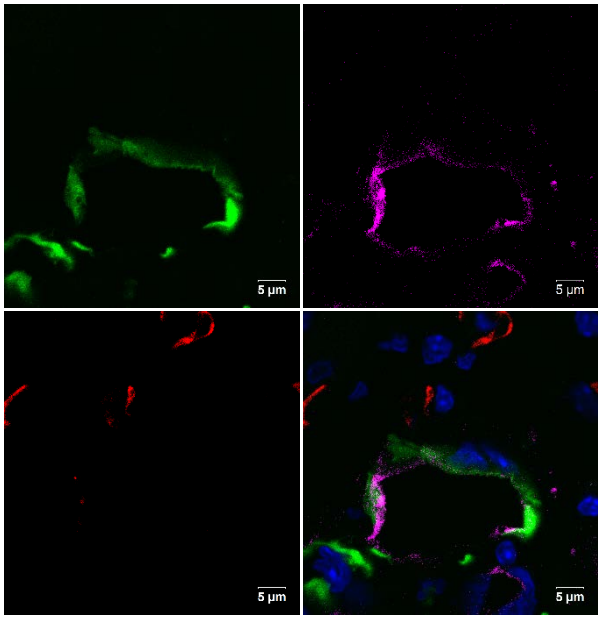

B

Human CD31/Mouse CD31/DAPI

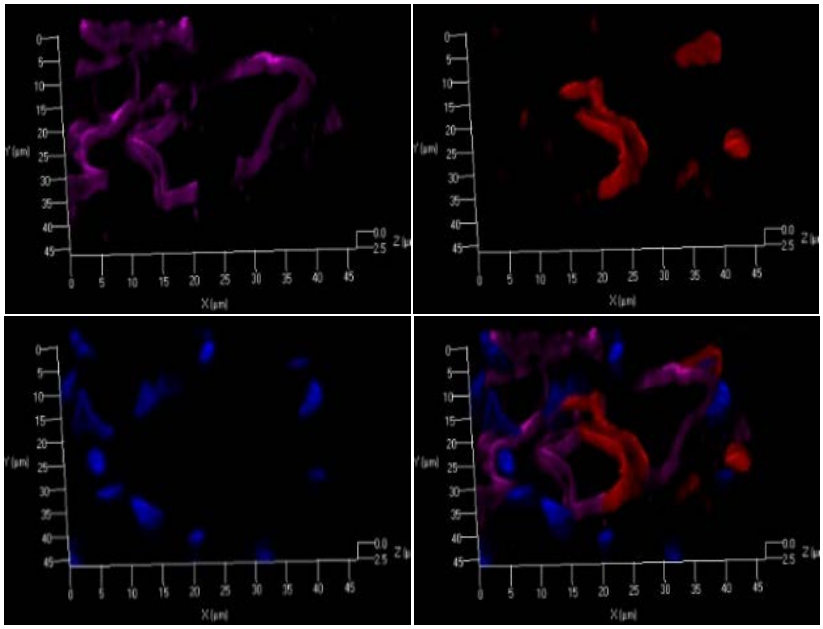

C

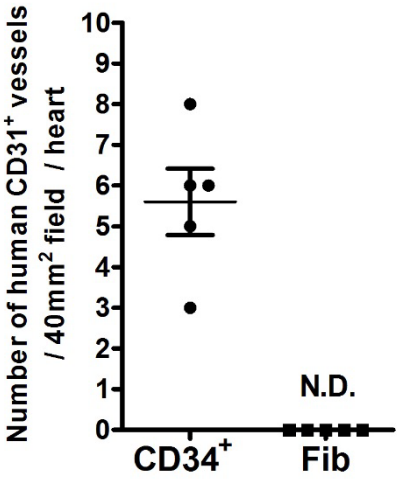

SUPPLEMENTAL FIGURE LEGENDS

Supplemental Figure 1. The morphology of human adult fibroblasts (**A**), De-differentiated fibroblasts at day 7 (**B**), iECs at day 10 (**C**) and induced erythroblasts at day 4(**D**). Scale bar: 50μm for **A**, **B**, and **C**; 100μm for **D**.

Supplemental Figure 2. Representative flow cytometry plots (**A**), and quantification and statistical analysis (**B**) of the endothelial surface marker CD31 and VE-cadherin in fibroblasts, $CD34^+$ progenitors, and iECs at day 10, (n=3). Representative flow cytometry plots of the erythrocyte marker CD235a and mesodermal markers CD34 (**C**), and quantification and statistical analysis of $CD235a^+$ (**D**) in fibroblasts, $CD34^+$ progenitors, and iErythroblasts at day 4, (n=3). Quantification of $CD34^+$ cells in VE-$cadherin^+$ iECs at day 10 and $CD235a^+$ iErythroblasts at day 4 (n=3) (**E**). Data are presented as mean ± SE, N.S. P>0.05, ** P<0.01, *** P<0.001, using one-way ANOVA in **B** and **D**.

Supplemental Figure 3. Quantitative PCR analysis of endothelial specific genes - *VE-cadherin* (**A**), *CD31* (**B**), *FLK1* (**C**), and *VWF* (**D**) in $CD34^+$ progenitors, CD31 sorted iECs at day 10 and HAECs. N=3. Data are presented as mean ± SE; *P<0.05, **P<0.01, N.S., p>0.05, using one-way ANOVA.

Supplemental Figure 4. The time course of trans-cell electrical resistance (TER) was measured for 180 minutes in fibroblasts, human aortic endothelial cells (HAECs) and iECs. Thrombin (3.5μg/ml;0.5 unit) was added as indicated. N=3.

Supplemental Figure 5. Quantitative PCR analysis of *OCT4* (**A**) and *c-MYC* (**B**) in fibroblasts, $CD34^+$ progenitor cells, and iECs (at day 10), n=3. Data are presented as mean ± SE; ***P<0.001, N.S. P>0.05; compared to fibroblasts, using one-way ANONA.

Supplemental Figure 6. (**A**) the schematic protocol of knocking down SOX17during the induction of iECs using lentivirus expressing SOX17shRNA or retrovirus expressing Sox17. (**B**-**C**) The infection efficiency of lentivirus expressing Sox17-1 shRNA in iECs– the representative flow cytometry plot (**B**) and quantitative and statistical analysis (**C**) of GFP expression in iECs. Data are presented as mean ± SE; ***P<0.001, compared to control cells (without infection), by Student's t-test. **(D)** Immunoblots of Sox17, VE-cadherin, and CD31 in the cells infected with lentivirus expressing scramble shRNA, Sox17-1 shRNA, Sox17-2 shRNA and Sox17-3 shRNA respectively.

Supplemental Figure 7. Representative confocal micrographs of immunohistochemistry staining of mouse liver with anti- Mouse TER119 (red, **A**), human CD235a (red, **B**) and anti- mouse VE-cadherin (green, **A** and **B**). Nucleus stained by DAPI. Scale bars, 100μm.

Supplemental Figure 8. *In vivo* angiogenesis of human aortic ECs. Representative confocal micrographs of immunohistochemistry staining of plugs with anti- human CD235a (red, **A**) or anti-mouse TER119 (red, **B**) and anti- human CD31 antibodies (green, **A** & **B**). Nuclei stained by DAPI. Scale bars, 5μm.

Supplemental Figure 9. Representative confocal micrographs of immunohistochemistry staining of plug of GFP expressed $CD34^+$ progenitor cells (green) with anti- TER119 (red). Nucleus stained by DAPI. Scale bars, 5μm.

Supplemental Figure 10. *Teratoma formation*. Representative gross images (**A**) and H&E staining images of explanted plugs at 8 weeks following implantation of iPSCs (**B**) and $CD34^+$ progenitor cells (**C**). Representative H&E staining images of primitive ectodermal neuroepithelium (**B1**), endodermal epithelium (**B2**) and mesodermal cartilage (**B3**) demonstrate teratomas in plugs containing iPSCs. Representative H&E staining

images of vessels (**C1**) in the section of angiogenesis plug. **(D)** The quantification and statistical analysis of teratoma formation of $CD34^+$ progenitor cells and iPSCs (n=5) shows no teratoma formation with $CD34^+$ cells.

Supplemental Figure 11. Representative confocal micrographs (**A**) of immunohistochemistry staining of anti-human CD31 (magenta) and anti-mouse CD31 (red) in myocardial cross-section at two weeks post MI with GFP expressed human $CD34^+$ progenitor treatment. Scale bars, 20μm (left) and 5μm (right). Representative 3D confocal micrographs (**B**) of integration of human vessels (anti-human CD31, magenta) and mouse vessels (anti-mouse CD31, red) in heart. Nuclei stained with DAPI (blue). The quantification and statistical analysis (**C**) of human vessels (human $CD31^+$, red) formed at two weeks post-MI with human $CD34^+$ progenitors or fibroblasts (n=5) treatment in the areas receiving cell injections. Data are presented as mean ± SE. N.D., not detected.

Supplemental Movie 1. A representative movie shows the reconstructed 3D structure using confocal image slices, thus demonstrating the integration of human UEA I+ vessels (red) formed by GFP-labeled fibroblast-derived CD34+ progenitors with mouse host GSIB4+ vessels (far red) in an explanted Matrigel plug. Nuclei were stained with DAPI. Width of each square: 10μm.

Supplemental Movie 2. A representative movie shows the reconstructed 3D structure using confocal image slices, thus demonstrating the integration of human CD31+ vessels (far-red) formed by fibroblast-derived CD34+ progenitors with mouse host CD31+ vessels (red) in the heart. Nuclei were stained with DAPI. Width of each square: 2.5μm.

References

1. Gong H, Rehman J, Tang H, Wary K, Mittal M, Chaturvedi P, Zhao YY, Komarova YA, Vogel SM and Malik AB. HIF2alpha signaling inhibits adherens junctional disruption in acute lung injury. *J Clin Invest*. 2015;125:652-64.
2. Zhang L, Malik S, Pang J, Wang H, Park KM, Yule DI, Blaxall BC and Smrcka AV. Phospholipase Cepsilon hydrolyzes perinuclear phosphatidylinositol 4-phosphate to regulate cardiac hypertrophy. *Cell*. 2013;153:216-27.
3. Tiruppathi C, Yan W, Sandoval R, Naqvi T, Pronin AN, Benovic JL and Malik AB. G protein-coupled receptor kinase-5 regulates thrombin-activated signaling in endothelial cells. *Proc Natl Acad Sci U S A*. 2000;97:7440-5.
4. Herbert BS, Hochreiter AE, Wright WE and Shay JW. Nonradioactive detection of telomerase activity using the telomeric repeat amplification protocol. *Nat Protoc*. 2006;1:1583-90.
5. Kang KT, Allen P and Bischoff J. Bioengineered human vascular networks transplanted into secondary mice reconnect with the host vasculature and re-establish perfusion. *Blood*. 2011;118:6718-21.